



Future Projections of Precipitation using Bias–Corrected High–Resolution Regional Climate Models for Sub–Regions with Homogeneous Characteristics in South Korea

Changyong Park¹ · Seok-Woo Shin¹ · Dong-Hyun Cha¹ · Myoung-Seok Suh² · Song-You Hong³ · Joong-Bae Ahn⁴ · Seung-Ki Min⁵ · Young-Hwa Byun⁶

Received: 31 May 2022 / Revised: 27 July 2022 / Accepted: 17 August 2022

© The Author(s) under exclusive licence to Korean Meteorological Society and Springer Nature B.V. 2022

Abstract

Although South Korea has a relatively small area when compared to neighboring countries, there are large differences in precipitation characteristics by region due to its complex topography. Therefore, to effectively respond to disasters caused by precipitation in South Korea, climate change information using a climate model with an improved spatial resolution is required. This study classified sub–regions with homogeneous characteristics in South Korea using transformed gridded precipitation observation datasets. Then, high–resolution regional climate models (RCMs) with a 12.5 km horizontal resolution, which are known to simulate added value well in simulating future projections of South Korea, were bias–corrected, and future changes in the precipitation means and extremes were analyzed using these RCMs. The classified precipitation sub–regions in South Korea reasonably reflected the observed distribution of precipitation, depending on latitude and topography. The future precipitation characteristics of the classified precipitation sub–regions were predicted using bias–corrected RCMs. While the annual precipitation is projected to increase relative to the present in most grids for all future periods, the RCP8.5 scenario for the mid–twenty-first century is projected to decrease in the north of the central region. Intensified warming in the late twenty-first century is predicted to considerably increase the mean precipitation intensity and magnitude of the high–intensity extreme precipitation in all the precipitation sub–regions. As these results can lead to increased hydrological disasters, this study will help to prepare practical countermeasures for precipitation changes on regional and local spatial scales in South Korea.

Keywords Precipitation · Future change · South Korea · Precipitation sub–region · Regional climate model · Bias correction

Responsible Editor: Hyemi Kim

✉ Dong-Hyun Cha
dhcha@unist.ac.kr

¹ School of Urban and Environmental Engineering, Ulsan National Institute of Science and Technology, 50 UNIST-gil, Eonyang-eup, Ulju-gun, Ulsan 689-798, Republic of Korea

² Department of Atmospheric Science, Kongju National University, Gongju, Chungnam, Republic of Korea

³ NOAA/ESRL/PSL and University of Colorado/CIRES, Boulder, CO, USA

1 Introduction

South Korea is highly exposed to natural disasters owing to the effects of the East Asian summer monsoon (EASM) rain band, heavy convective rains, and tropical cyclones in

⁴ Division of Earth Environmental System, Pusan National University, Busan, Republic of Korea

⁵ Division of Environmental Science and Engineering, Pohang University of Science and Technology, Pohang, Gyeongbuk, Republic of Korea

⁶ National Institute of Meteorological Sciences, Seogwipo, Jeju, Republic of Korea

summer. In particular, South Korea has a relatively small area when compared to neighboring countries (e.g., China or Japan) but it has significant regional differences in its precipitation characteristics due to its complex topography. As a result, the pattern of disasters that occur varies by watershed and region due to additional factors such as population density and the location of various industrial facilities (Ministry of Environment 2020). Therefore, climate change information using a climate model with improved spatial resolution is required for effective mitigation and adaptation to climate change on regional or local spatial scales.

The global climate model (GCM), which targets the global scale, has a spatial resolution of several hundred kilometers; therefore, there is a limit to obtaining information on future climate change at regional or local spatial scales (Park et al. 2020a). Therefore, to resolve the insufficient future climate simulation of GCMs on regional or local spatial scales, the Coordinated Regional Climate Downscaling Experiment (CORDEX) project was established by the World Climate Research Programme (WCRP). In the CORDEX project, diverse regional climate models (RCMs) were produced to provide quality-controlled information for regional climate change in 14 regional domains (Giorgi et al. 2009; Park et al. 2020a, 2021; <http://wcrp-cordex.ipsl.jussieu.fr/>). Currently, for the East Asia domain, the CORDEX East Asia project team is producing RCMs with various spatial resolutions forced by multi-GCMs to project future East Asian climate information. In phase I, RCMs with a 50-km horizontal resolution covering East Asia were first produced, followed by RCMs with enhanced horizontal resolution (12.5 km) covering far East Asia centered on the Korean Peninsula. The reason for the additional development of the RCMs with 12.5 km high resolution is that RCMs with 50 km horizontal resolution are insufficient to reproduce or project more useful climate information (e.g., agriculture and hydrology) on a fine spatial scale (Cha et al. 2016; Oh et al. 2016; Suh et al. 2016; Kim et al. 2018; Park et al. 2020a). Several studies have been conducted using these multi-RCMs with a 12.5 km horizontal resolution for future climate projections and model evaluations covering South Korea (Ahn et al. 2016; Cha et al. 2016; Choi et al. 2016; Oh et al. 2016; Suh et al. 2016; Lee et al. 2017a; Kim et al. 2018; Park et al. 2020a).

This study is a follow-up study to the one conducted by Park et al. (2021), which targeted East Asia. We classified regions with homogeneous precipitation characteristics referenced in the present, targeting South Korea. Park et al. (2021) used multi-RCMs from CORDEX phase I with a resolution of 50 km suitable for the future precipitation projections of classified precipitation sub-regions. When these RCMs are applied to predictions of future precipitation for classified precipitation sub-regions on the South Korean scale, the grid size is large, so there are limitations in the

production of future climate change information. Therefore, this study has applied 12.5 km high-resolution multi-RCMs produced in the same project to predict the future precipitation of classified precipitation sub-regions in South Korea. These RCMs are known to simulate the added value well in future projections on the scale of South Korea (Park et al., 2020a). Moreover, this study suggests various possibilities for responding to precipitation in South Korea in the future according to the magnitude of future warming by additionally applying the representative concentration pathways (RCP)2.6 scenario corresponding to the Paris Agreement.

The remainder of this paper is organized as follows. The observation dataset, model simulations, and main analysis methods are introduced in Section 2. For the classified precipitation sub-regions in South Korea, climatology characteristics from the observations and future precipitation characteristics using the bias-corrected RCM datasets are investigated in Section 3. Finally, a summary and conclusions are presented in Section 4.

2 Data and Experiments

2.1 Observation and Model Simulations

Regarding the research data, the main difference from Park et al. (2021) is that this study applied data from the Korea Meteorological Administration (KMA) for observation and improved the spatial resolution data for the regional climate models. We selected the land area of South Korea as the analysis domain. From observational data and RCMs, the major variables applied in this study were daily precipitation datasets. Climate datasets of 73 Automated Synoptic Observing System (ASOS) stations for 25 years from 1981 to 2005 period were used to classify the current precipitation sub-regions in South Korea. In addition, the ASOS observational dataset was used as reference data for the bias correction of the RCMs. Simulated RCM datasets with a 12.5 km high horizontal resolution, which cover Far-East Asia centered on the Korean Peninsula, participating in the CORDEX East Asia project, were used to project the future precipitation characteristics for each identified precipitation sub-region in South Korea. These RCMs were forced by two of the Coupled Model Intercomparison Project 5 GCMs (HadGEM2-AO and MPI-ESM-LR), which showed relatively good simulation performance in capturing the observed East Asian climate characteristics (Martin et al. 2011; Baek et al. 2013; Sperber et al. 2013; Guo et al. 2016). We projected future precipitation characteristics using five RCMs (HadGEM3-RA, RegCM4, SNURCM, WRF, and GRIMs) forced by HadGEM2-AO GCM, which were simulated until the late twenty-first century,

the period of this study. The future projection period is the 2041–2065 period for the mid-twenty-first century and the 2075–2099 period for the late twenty-first century. The same number of analysis years (25 years) as the present was applied for objective comparison. The configurations of the five RCMs are presented in Table 1. Multi-model ensemble (MME) datasets were employed for all RCM experiments (historical, RCP2.6, and RCP8.5) by averaging the unweighted output produced by five RCM simulations. The historical experiment was used to evaluate RCM’s performance to each identified precipitation sub-region for the 1981–2005 period in South Korea and as the reference dataset for the future precipitation change projections. The RCP2.6 scenario is the closest to the response of the Paris Agreement among the RCP greenhouse gas emission scenarios, and RCP8.5, a *business as usual* (BAU) scenario, maintains greenhouse gas emissions at the present level. In this study, these conflicting scenarios were applied to predict the future precipitation characteristics for each precipitation sub-region identified by observation and to classify future precipitation sub-regions.

2.2 Analysis Methods

Because the ASOS datasets are point data, spatially non-uniform data were converted into gridded data with uniform characteristics to perform bias correction of regional climate models and comparison with RCMs. We applied the Barnes technique to these dataset’s conversions and extracted only the land area of South Korea. Based on the gridded ASOS datasets, only the land area of South Korea was analyzed even for RCMs. The Barnes technique determines the values of each grid by assigning weights to the positions of the observations at the center of the grid to be analyzed. This is an effective method for calculating results when there are no appropriate reference values (Barnes 1964; Koch et al. 1983; Lee et al. 2017b; Park et al. 2020b). The initial estimate (g_0) of the grid is determined by N observations (f) within the effective radius (c) and the weight (w_m), which is inversely

proportional to the square of the grid-observed distance (r_m) (Koch et al. 1983).

$$g_0(i, j) = \frac{\sum_{m=1}^N w_m f(x_m, y_m)}{\sum_{m=1}^N w_m} \tag{1}$$

$$w_m = \exp\left(\frac{-r_m^2}{c^2}\right) \tag{2}$$

The final estimated value of the grid point is (g_1), and (γ) is a numerical convergence parameter with $0 < \gamma < 1$ that adjusts the difference between (w'_m) and (w_m) to include small-scale information.

$$g_1(i, j) = g_0(i, j) + \frac{\sum_{m=1}^N w'_m [f(x_m, y_m) - g_0(x_m, y_m)]}{\sum_{m=1}^N w'_m} \tag{3}$$

$$w'_m = \exp\left(\frac{-r_m^2}{\gamma c^2}\right) \tag{4}$$

We then bias-corrected the high-resolution regional climate models using the gridded ASOS observation datasets. Because the model performance is improved when the bias correction technique is applied to the climate model, the number of cases in which it is applied to climate change research using climate models has been increasing in recently years (Yan et al. 2015; Maraun et al. 2017; Kim et al. 2020, 2021; Park et al. 2021). The quantile mapping for the entire period (QME), which applied quantile mapping to daily precipitation, was applied as a bias correction technique. The quantile mapping method is suitable for precipitation as a method of correcting data for 0 mm days of daily precipitation by comparing the cumulative distribution function (CDF) of the observations and models. We also applied the quantile mapping method to CDF for bias correction (Kim et al. 2020). The CDF applies the generalized extreme value (GEV) distribution, and variable x is as follows:

Table 1 Configurations of the RCMs used in this study

	HadGEM3-RA	RegCM4	SNURCM	WRF	GRIMs
Number of grid points, (latitude × longitude)	184 × 164	198 × 178	199 × 179	201 × 180	201 × 182
Vertical levels	Hybrid-38	σ-23	σ-24	σ-27	σ-28
Dynamic framework	Non-hydrostatic	Hydrostatic	Non-hydrostatic	Non-hydrostatic	Hydrostatic
Convection scheme	Revised mass flux scheme	MIT-Emanuel	Kain-Fritsch II	Kain-Fritsch II	Simplified Arakawa-Schubert
Land surface	MOSES-II	CLM3.5	CLM3.0	Noah	Noah
References	Davies et al. (2005)	Giorgi et al. (2012)	Cha and Lee (2009)	Skamarock et al. (2005)	Hong et al. (2013)

$$F(x; \mu, \sigma, \xi) = \begin{cases} \exp\left[-\exp\left\{-\frac{x-\mu}{\sigma}\right\}\right], \xi = 0 \\ \exp\left[-\left\{1 + \xi\frac{x-\mu}{\sigma}\right\}^{-\xi^{-1}}\right], \xi \neq 0, 1 + \xi\frac{x-\mu}{\sigma} > 0 \end{cases} \tag{5}$$

where μ , σ , and ξ are the location, scale, and shape parameters, respectively, which were estimated following the L-moments. The CDF of each RCM, estimated using daily precipitation values from the historical experiment, was fitted to that of the observation dataset.

$$P_{Hist}^*(d) = F_{obs}^{-1}\left(F_{Hist}\left(P_{Hist}^{*1}(d)|\alpha_{Hist}, \beta_{Hist}, \gamma_{Hist}\right)|\alpha_{obs}, \beta_{obs}, \gamma_{obs}\right) \tag{6}$$

$$P_{RCP}^*(d) = F_{obs}^{-1}\left(F_{Hist}\left(P_{RCP}^{*1}(d)|\alpha_{Hist}, \beta_{Hist}, \gamma_{Hist}\right)|\alpha_{obs}, \beta_{obs}, \gamma_{obs}\right) \tag{7}$$

Here, P , F , $Hist$, and RCP were defined as precipitation, CDF, historical experiment, and RCP scenario, respectively. For sub- or superscripts, ‘*’ and ‘*1’ indicated the final bias-corrected result and bias-corrected dataset of an intermediate step (Kim et al. 2020).

We applied Ward’s hierarchical clustering method as a statistical technique (Ward 1963) to identify the present and future precipitation sub-regions in South Korea. Ward’s method is widely applied to classify climatic zones (Park et al. 2009, 2021; Bieniek et al. 2012; Awan et al. 2015). Ward’s hierarchical clustering method minimizes the increase in the error sum of squares, which is proportional to the squared Euclidean distance between i and j cluster centers (Murtagh and Legendre, 2014). The clustering method used in this study is the same as that applied in the previous study; therefore, further details of Ward’s technique can be referred to in Park et al. (2021).

Four precipitation indices from the Statistical and Regional Dynamical Downscaling of Extremes (STARDEX, <https://crudata.uea.ac.uk/projects/stardex>) and Expert Team on Climate Change Detection and Indices (ETCCDI, http://etccdi.pacificclimate.org/list_27_indices.shtml) were selected to examine the precipitation extremes of each classified sub-region in South Korea (Table 2). These indices were analyzed by dividing them into the low-intensity extreme precipitation indices of PQ90 and SDII and the high-intensity extreme precipitation indices of RX1 day and

Table 2 Extreme precipitation indices used in this study

Index	Definition (unit)
RX1day	Maximum 1-day precipitation amount (mm)
RX5day	Maximum 5-day precipitation amount (mm)
PQ90	90th percentile of precipitation on days with > 1 mm precipitation (mm)
SDII	Total precipitation amount/number of $R \geq 1$ mm (mm d^{-1})

RX5day. For drought, a standard precipitation index (SPI) was applied. The SPI is the most widely used drought index and is designed to quantify the precipitation deficit over several timescales to reflect the effect of droughts on the availability of various water resources. Monthly precipitation values were fitted to a 2-parameter gamma or Pearson type III distribution and then transformed to a normal distribution to obtain the SPI (Mckee et al. 1993; Guttman 1999; Hayes et al. 1999, 2011; WMO 2012; Bothe et al. 2012; Trenberth et al. 2014; Choi et al. 2016; Myoung et al. 2020; An et al. 2022; Lee et al. 2022). Therefore, the average SPI is zero, and the relative degree of the droughts can be evaluated according to the climatic characteristics of each region. The classification scale presented in Table 3 was used to determine drought intensity (Mckee et al. 1993; WMO 2012). According to this scale, a drought event occurs when the SPI reaches an intensity of -1.0 or less. The KMA officially evaluates meteorological drought in South Korea using the SPI based on 6-month precipitation (Lee et al. 2020; <https://hydro.kma.go.kr/drought/obsAdm.do>). Moreover, in South Korea, the SPI with a gamma distribution performs better than a Pearson type III distribution (Yoo et al. 2013; Lee et al. 2022). Accordingly, this study predicted droughts in the future scenarios by calculating the number of months with an SPI of -1.0 or less with a gamma distribution according to 6-month precipitation, and the dry seasons of winter and spring (December to May) were targeted.

3 Results

3.1 Climatology Characteristics of the Classified Precipitation Sub-Regions in South Korea

In this section, we examine the climatology characteristics of annual and daily precipitation for each sub-region of South Korea classified by observation. Figure 1(a) shows the annual precipitation distribution from 1981 to 2005 in South Korea. The mean annual precipitation in South Korea over 25 years is 1,332 mm, ranging from less than 1,000 mm on Baengnyeong Island to over 1,800 mm

Table 3 SPI values

Value	Drought intensity
2.0+	Extremely wet
1.5 to 1.99	Very wet
1.0 to 1.49	Moderately wet
-0.99 to 0.99	Near normal
-1.0 to -1.49	Moderately dry
-1.5 to -1.99	Severely dry
-2 and less	Extremely dry

Fig. 1 Spatial distributions of (a) annual precipitation (mm) and (b) classified precipitation sub-regions using gridded precipitation observation for South Korea. In (a), “am” and “sd” represent the areal mean for the annual precipitation in South Korea and its standard deviation, respectively

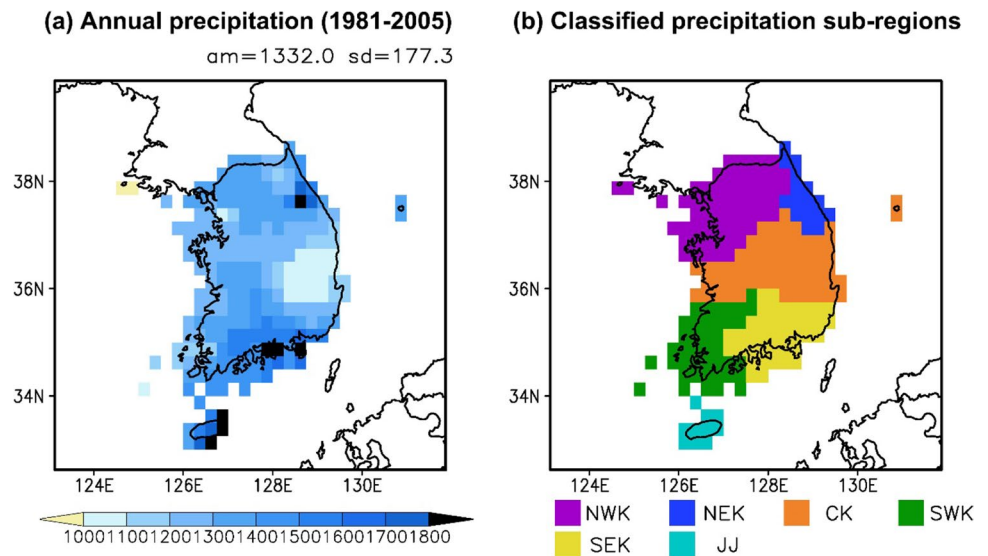


Table 4 Abbreviations of the classified precipitation sub-regions

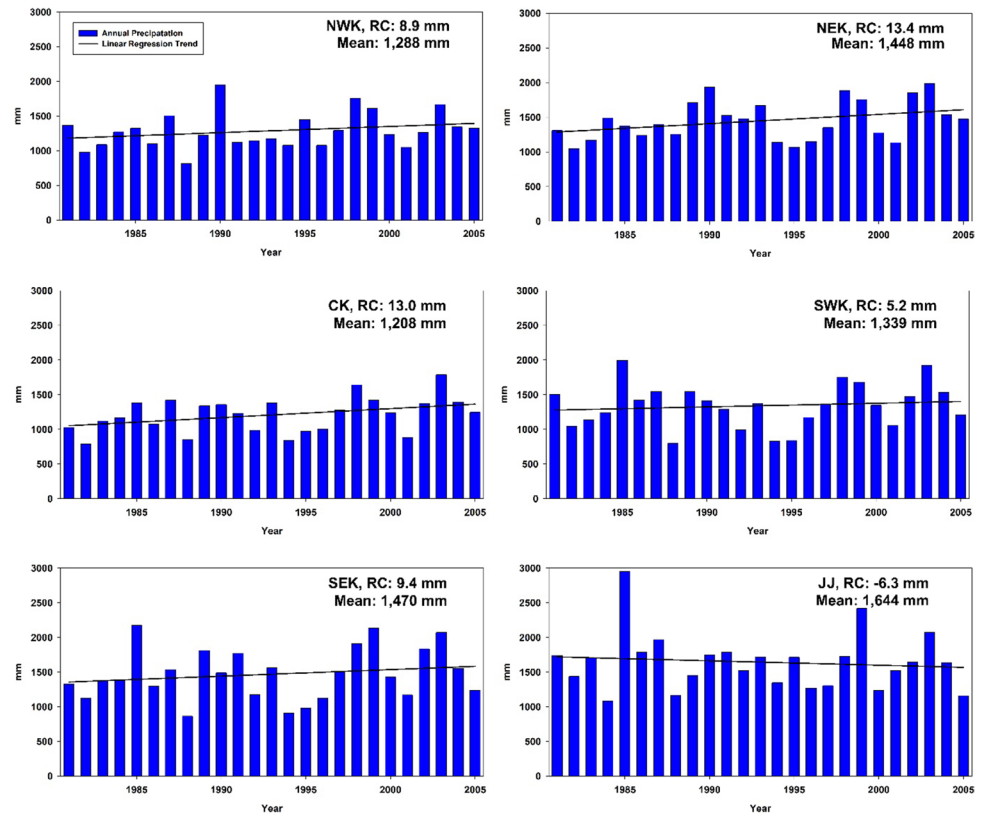
Abbreviation	Definition
NWK	Northwestern Korea
NEK	Northeastern Korea
CK	Central Korea
SWK	Southwestern Korea
SEK	Southeastern Korea
JJ	Jeju

on the eastern part of Jeju-do and the southern coast. Gyeongsangbuk-do has relatively little precipitation, with an annual precipitation of less than 1,100 mm due to topographical effects. Chang and Ding (2005) and Wilks (2011) suggested that the appropriate number of clusters requires the subjective selection of an expert with sufficient prior knowledge according to the purpose of the analysis. Therefore, we selected six as the appropriate number of clusters using the gridded ASOS dataset (Fig. 1(b)). This precipitation classification result seems to reasonably reflect the observed distribution of annual precipitation, depending on latitude and topography. The classified sub-regions are named according to their location and geographical name, and the abbreviations are presented in Table 4. For example, the NWK sub-region represents the northwestern region of South Korea, and the JJ sub-region represents the Jeju-do region. Zonally, South Korea was divided into four regions, and the northern and southern regions were further classified into east-west regions. In the northern part of South Korea, the sub-regions are divided into NWK and NEK sub-regions based on the *Taebaek* Mountains, which are the largest mountains in South Korea. The NEK sub-region adjacent to the east coast

is an exit location for typhoons that affect South Korea in summer, and it is also a region where a record heavy rainfall of 870.2 mm for daily precipitation occurred during Typhoon *Rusa* in 2002. Furthermore, it is a snowy region where a large amount of snow falls due to the influence of the *Taebaek* Mountains when the east wind has an effect in winter. That is, when compared with metropolitan areas of the same latitude, the NEK sub-region has a large difference in precipitation characteristics owing to the influence of a large-scale mountain range. The southern region of South Korea is also divided into the SWK and SEK sub-regions based on the *Sobaek* Mountains, and these regions are almost identical to the administrative districts of Jeolla-do and Gyeongsang-do, respectively. When the northern Siberian high expands in winter, the large amount of snow in the SWK sub-region is due to the influence of the *Sobaek* Mountains. The SEK sub-region often corresponds to the entrance when typhoons land in South Korea (Choi and Kim 2007; Park et al. 2008).

Figure 2 shows the temporal variations and linear regression trends of annual precipitation during the 1981–2005 period for the classified sub-regions, where RC is the regression coefficient. The mean annual precipitation for the 25 years from 1981 to 2005 was the highest in the JJ sub-region at 1,644 mm and the lowest in the CK sub-region at 1,208 mm. The JJ sub-region seems to have the most precipitation due to the frequent effects of the EASM rain belt and typhoons in the summer. The linear regression trend in all regions did not show a statistically significant trend as the p-value was greater than 10 in all regions. The annual precipitation tended to increase in the five sub-regions. In particular, the NEK sub-region showed the most significant increasing trend out of all the sub-regions. This is due to the large amount of precipitation from two typhoons (*Rusa* and

Fig. 2 Time series of annual precipitation for each precipitation sub-region from gridded precipitation observation for South Korea. RC is an abbreviation for the regression coefficient



Maemi) that hit the area in 2002 and 2003, respectively. The JJ sub-region, with the largest annual precipitation, showed a decreasing trend.

Furthermore, the temporal variations in the climatological daily precipitation formed during the 1981–2005 period for the classified sub-regions (Fig. 3). Summer on the Korean Peninsula is the season when precipitation is concentrated under the influence of the EASM rain belt called the “rainy season”. Two peaks in summer were well expressed in all the classified sub-regions. These

peaks were associated with the onset and withdrawal of the northward movement of the EASM rain belt from June to August (Park et al. 2021). In most regions, the precipitation at the first peak of the two peaks was large; however, in the NEK sub-region, the second peak had more precipitation than the first. As previously mentioned, this is because the climatological monthly precipitation in September was larger than that in other regions due to the influence of the two strong typhoons in the NEK sub-region.

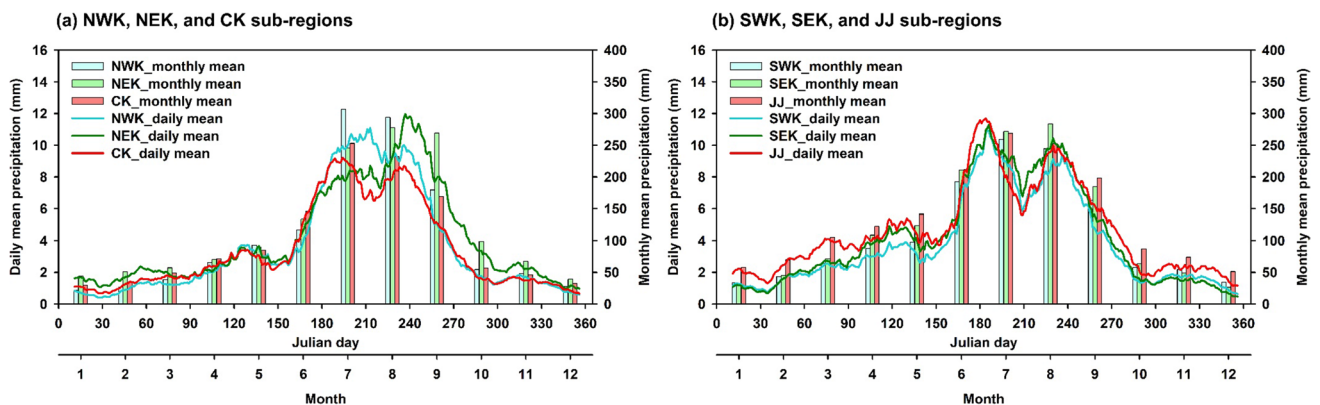


Fig. 3 Temporal variations in the climatological daily precipitation for (a) NWK, NEK, and CK, and (b) SWK, SEK, and JJ precipitation sub-regions

3.2 Future Precipitation Characteristics of the Classified Precipitation Sub-Regions in South Korea

A performance evaluation of the historical experimental datasets is required before estimating the future projections of precipitation in each classified region. Because bias-corrected RCMs were applied in this study, the performances of bias-corrected and non-bias-corrected RCMs were compared in the historical experiment using a Taylor diagram to evaluate the effect of bias correction on the annual precipitation of each classified sub-region (Fig. 4). The KMA ASOS datasets were used as reference data. A reference point with a standard deviation and correlation coefficient of one is the point that indicates a perfect model performance. The distance from each model point to the reference point denotes the model errors related to spatial patterns (Taylor 2001). For non-bias-corrected RCMs, the overall model performance was low in all sub-regions. The RCMs and MME of the JJ sub-region were the best, and some RCMs of the CK, SEK, and NEK sub-regions showed negative correlation coefficient values. In contrast, all five bias-corrected RCMs and their MME are close to the reference point for all sub-regions, denoting a near-perfect spatial-pattern RCM performance. This result shows the usefulness of bias-corrected RCMs and provides strong evidence that it is appropriate to apply bias-corrected RCMs to future precipitation projections for each classified sub-region in South Korea.

The RCM MME distributions of the period-averaged annual precipitation and its future projections in South Korea according to the scenario for two future periods (2041–2065, 2075–2099) are shown in Fig. 5. Here, future projections of annual precipitation are expressed as percentages. To indicate inter-model agreements for the simulated data sets, the hatched marking indicates areas where all five RCMs have the same sign. Future annual precipitation patterns tend to be similar for the scenarios RCP2.6 and RCP8.5. As considerable precipitation is expected on the south and northeast coasts and a little precipitation in Gyeongsangbuk-do, the scenarios seem to show a similar pattern to the present. In the case of the area-averaged annual precipitation, the RCP2.6 scenario predicted precipitation to decrease by 4.3% in the 2075–2099 period compared to the 2041–2065 period. In contrast, the RCP8.5 scenario predicted precipitation to increase by 16.5%. The RCP8.5 scenario predicted that there will be less precipitation in the 2041–2065 period than in the RCP2.6 scenario, but there will be more precipitation with a large difference in the 2075–2099 period. In particular, it is predicted that an area showing 1,800 mm year⁻¹ or more is expected to expand on the southern coast and Jeju region in the RCP8.5 scenario for the 2075–2099 period. As for the spatial distribution of future projections compared to the present, the RCP2.6 scenario will have an overall positive value and is expected to show a “south-high-north-low” distribution in the 2041–2065 period. In the 2075–2099 period compared to

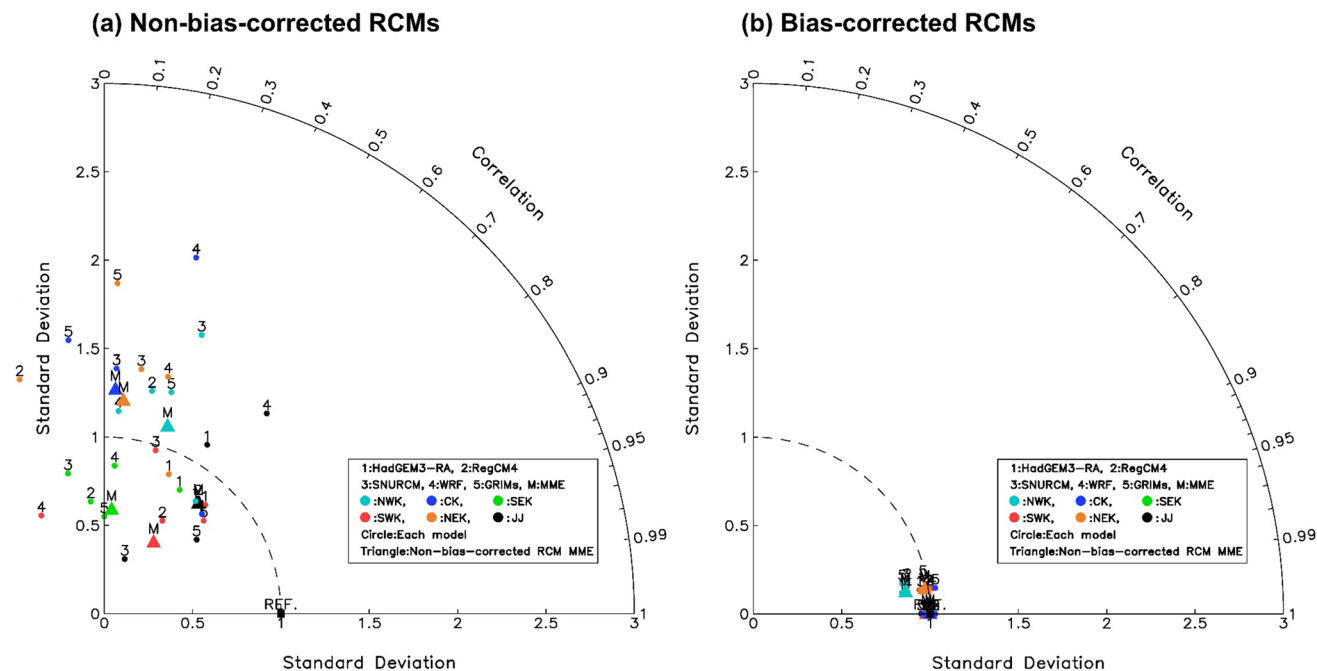


Fig. 4 Taylor diagram for (a) the non-bias-corrected and (b) bias-corrected RCMs of the Historical experiment for each sub-region

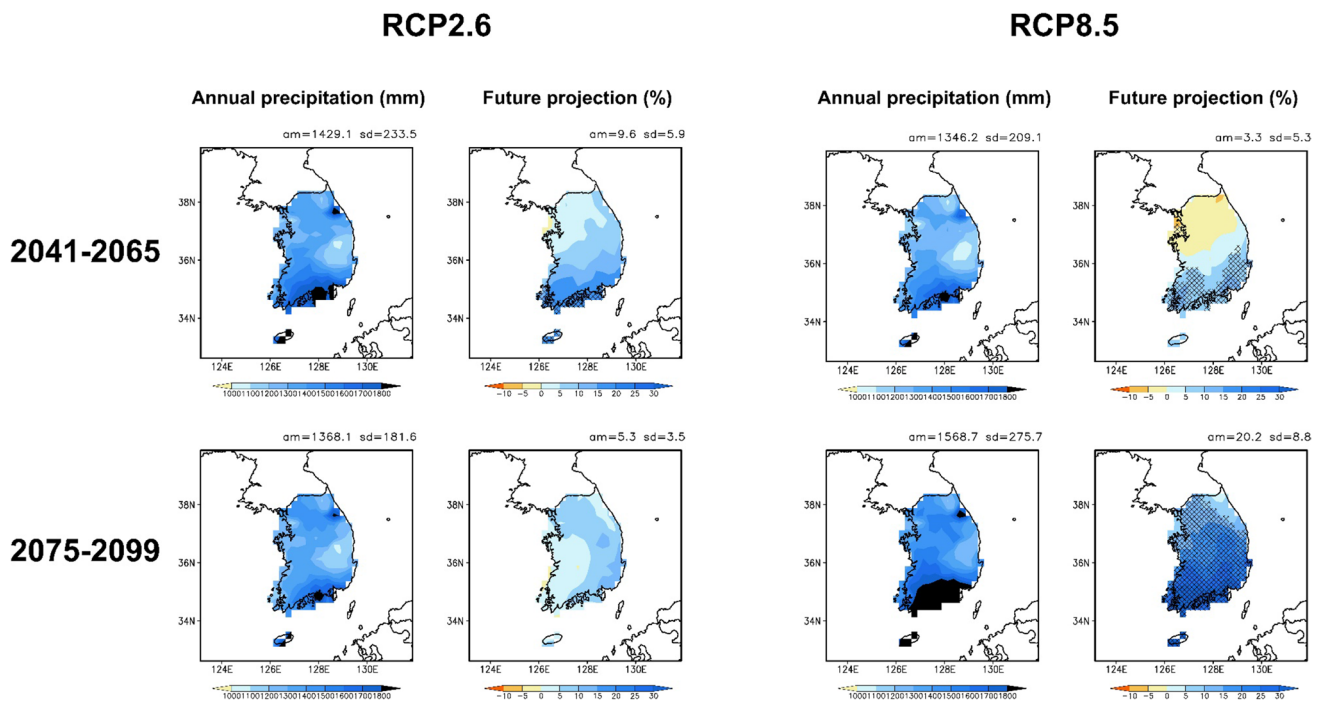


Fig. 5 Spatial distributions of future scenarios for future annual precipitation and its change for the RCM MMEs. In the upper right corner of the figures, “am” and “sd” represent the areal mean for

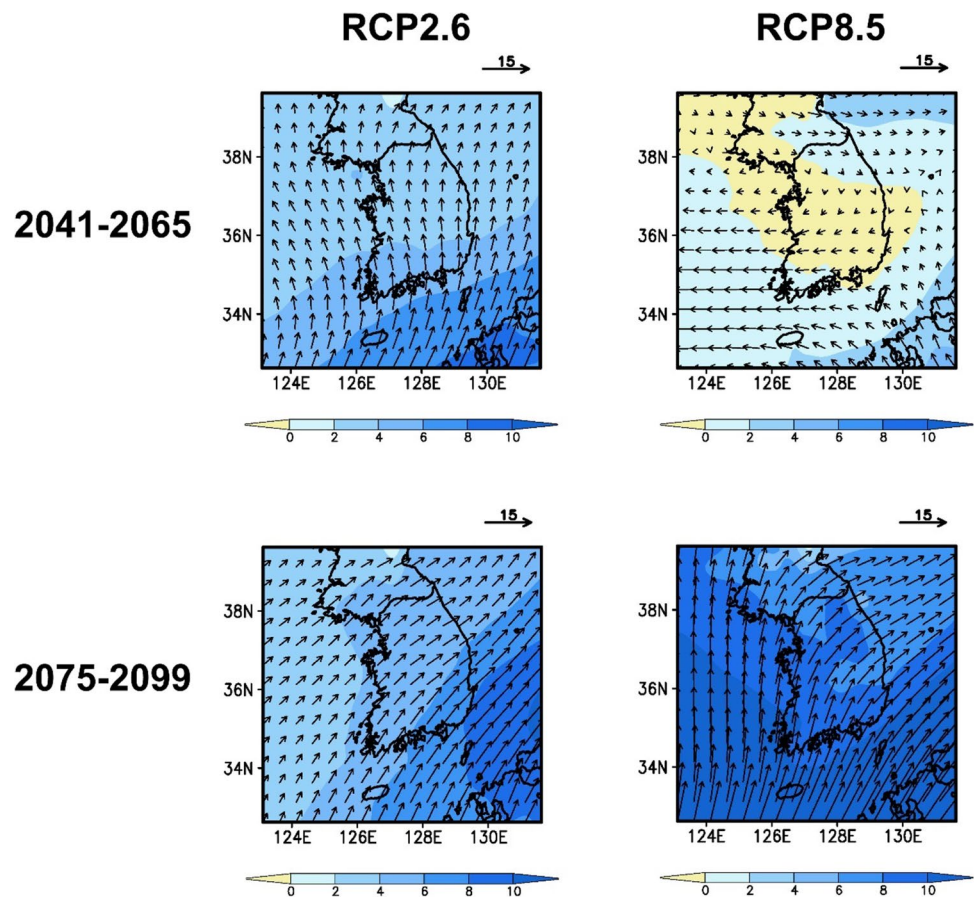
future annual precipitation in South Korea and its standard deviation, respectively. In columns 2 and 4, the hatched marking indicates areas where all RCMs have the same sign

the previous period, the rate of increase was expected to increase in the northern region but decrease in the southern part for the RCP2.6 scenario. From the projections of the RCP2.6 scenario in the two future periods, most grids of South Korea did not show good inter-model agreements. For RCP8.5, the average annual precipitation in the north of the central region is projected to decrease compared to that in the 2041–2065 period, and it will increase in the south and central regions. In the 2075–2099 period, the entire region of South Korea has a positive projection with a “south–high–north–low” distribution. Remarkably, some parts of the southern coastal region are predicted to have an increase in precipitation by more than 30% compared with that in the present. In the case of the RCP8.5 scenario, good model agreements were found in the southern part and the western NWK sub–region in the 2041–2065 period, and in most regions except for the NEK sub–region in the 2075–2099 period. These future precipitation changes are related to variations in moisture transport in low–level atmospheres. To briefly analyze the factors influencing these future precipitation projections in South Korea, we investigated the future changes in the moisture flux and its magnitude in the low–level atmosphere during the summer season (June–July–August), when precipitation is concentrated (Fig. 6), and the results were generally similar to the distribution of future projections for period–averaged annual precipitation in Fig. 5.

In Fig. 6, the moisture flux magnitude is calculated as the square root of the quadratic sum of the moisture transport (Sepulchre et al. 2010; Park et al. 2021). From the RCP2.6 scenario in the two future periods, and RCP8.5, in the 2075–2099 period, the moisture flux magnitude is expected to increase in all grids of South Korea as the inflow of moisture from the warm and humid low–latitude ocean into South Korea’s inland increases. In contrast, in RCP8.5, for the period 2041–2065, the moisture flux magnitude is expected to decrease in the broad grids except for the northeast, southwest, and Jeju regions.

The projection of the extreme precipitation index for each classified precipitation sub–region and South Korea was analyzed by dividing it into low– and high–intensity regions (Fig. 7). Most notably, in the case of the RCP8.5 scenario with the largest warming scale, the high–intensity extreme precipitation indices are predicted to increase more than the low–intensity extreme precipitation indices in most sub–regions during the 2070–2099 period. This may be related to the stronger contribution of increasing moisture content to more extreme precipitation in the Clausius–Clapeyron relationship and convective precipitation intensification in the high–emission CO₂ scenario (Kim et al. 2018; Lee et al. 2018; Park et al. 2021). This result suggests that the intensification of warming causes a large increase in high–intensity extreme precipitation, suggesting that precipitation disasters in South Korea may increase;

Fig. 6 Spatial distributions of the future changes in horizontal moisture flux (vector) and its magnitude (shading) at 850 hPa ($\text{g kg}^{-1} \text{m s}^{-1}$) during the summer season for the RCM MMEs



therefore, a firmer policy for mitigating and responding to climate change is required.

For the low-intensity extreme precipitation indices, the RCP2.6 scenario is projected to have positive projections for all the regions during the two future periods. Overall, the RCP2.6 scenario during 2041–2065 period and RCP8.5 scenario during 2075–2099 period are predicted to have large projections. SDII indicates precipitation intensity. By taking into account the number of days with a rainfall of larger than 1 mm day^{-1} , the number of precipitation days is predicted to decrease in the high-latitude sub-regions of NWK and NEK and increase in the low-latitude sub-regions of SEK, SWK, and JJ in both scenarios during the 2041–2065 period (Fig. S1). The 2075–2099 period is predicted to decrease in the NWK and NEK sub-regions of the two scenarios and in the CK and SWK sub-regions of the RCP2.6 scenario. In contrast, the SDII is expected to increase in all regions, scenarios, and periods. Notably, during the 2075–2099 period, the SDII is expected to increase significantly in RCP8.5, a high-emission scenario, and will be distributed in the fashion of “south-high-north-low”. These results show that strengthened warming leads to an increase in the mean precipitation intensity, which more strongly supports the association with the Clausius-Clapeyron relationship

presented above. PQ90, which belongs to another low-intensity extreme precipitation category, is generally similar to the SDII, except for the negative projection of RCP8.5, during the 2041–2065 period in some sub-regions. In the case of high-intensity extreme precipitation indices, the common characteristics of all sub-regions during the 2041–2065 period did not appear, but in the 2075–2099 period, the RCP8.5 scenario showed a larger projection than the RCP2.6 scenario in all sub-regions. Similar to the low-intensity extreme precipitation indices, a large increase in the RCP8.5 scenario was expected during the 2075–2099 period and this will be distributed in the fashion of “south-high-north-low”.

Moreover, we quantitatively predicted future droughts during the dry season (winter and spring) for each sub-region and South Korea (Fig. 8). For the projection of the number of months with an SPI of -1.0 or less, the areal mean value of South Korea for the two future scenarios in the two future periods is projected from -0.1 to -0.2, not significantly different from the present (Fig. S2). Increases in the East Coast region and decreases elsewhere are predicted consistently in the two future scenarios in the two future periods. For the classified precipitation sub-regions, the NWK, CK, and SWK sub-regions are predicted to have

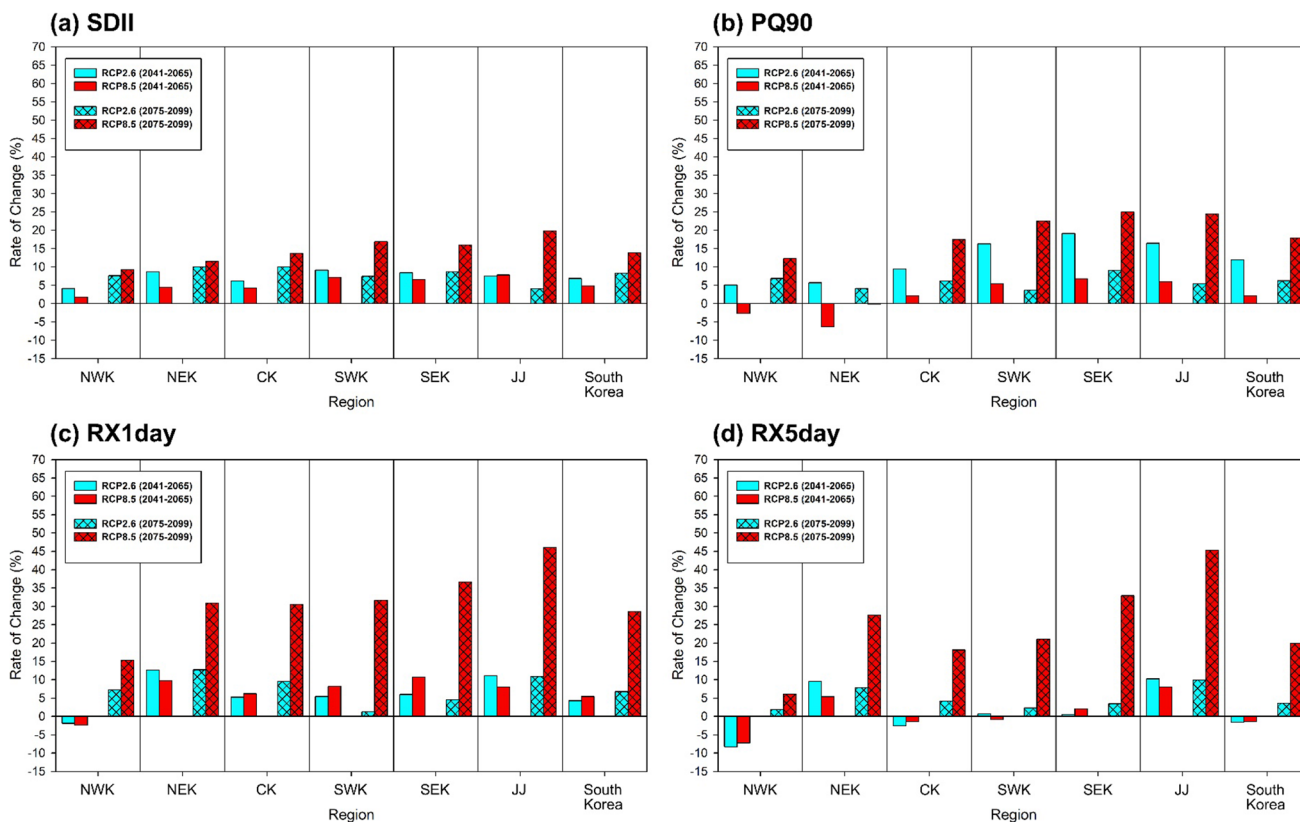
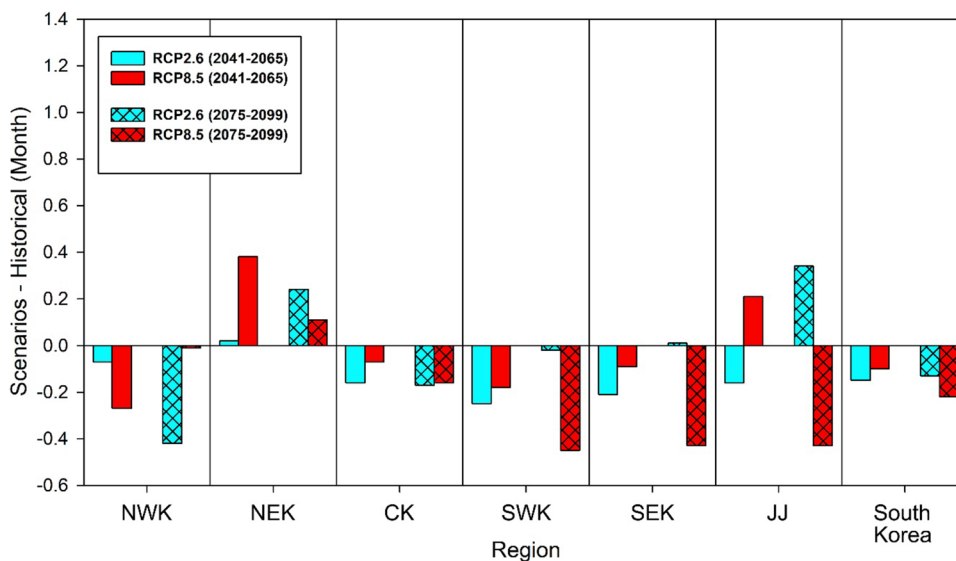


Fig. 7 Future RCM MME changes in (a and b) low-intensity extremes and (c and d) high-intensity indices for each precipitation sub-region and South Korea

Fig. 8 Future RCM MME changes in the number of months with an SPI of -1.0 or less during the dry season for each precipitation sub-region and South Korea



fewer drought months than the present in the two future scenarios in the two future periods. In contrast, the NEK sub-region, located in the east coast region, differs significantly from other sub-regions in that drought months are expected to increase in the two future scenarios in the two future periods. These results for future drought projections

for South Korea are mostly inconsistent with the results of the precipitation forecast presented above. This is because of the concentration of precipitation in summer and the drought that occurs mainly from winter to spring, which is the dry season, that is, the seasonal difference between the occurrence of the two events.

4 Summary and Conclusions

In this study, a follow-up of the study by Park et al. (2021) classified sub-regions with homogeneous precipitation characteristics in the South Korean domain using transformed into gridded precipitation observation datasets. Moreover, future changes in precipitation means and extremes were analyzed using bias-corrected RCMs. The classified precipitation sub-regions in South Korea reasonably reflected the observed distribution of annual precipitation, depending on latitude and topography. The observed annual precipitation of the classified sub-regions tended to increase in five sub-regions, but not significant trends. Owing to the onset and withdrawal of the EASM rain belt, two peaks in summer were well demonstrated in all classified sub-regions.

As the usefulness of the bias-corrected RCM was demonstrated, we applied the bias-correction technique to future precipitation scenarios. The future annual precipitation compared to the present was projected to have a positive value in most grids for the RCP2.6 scenario in the two future periods and for the RCP8.5 scenario in the 2075–2099 period. Meanwhile, the RCP8.5 scenario in the 2041–2065 period was predicted to have a decrease compared to the present in the north of the central region. These results are related to moisture transport projections in the low-level atmosphere. In the projection of the extreme precipitation index, for the RCP8.5 scenario with the largest warming scale, high-intensity extreme precipitation indices were predicted to increase more than low-intensity extreme precipitation indices in most sub-regions in the late twenty-first century. Moreover, intensified warming in the late twenty-first century has been projected to considerably increase the mean precipitation intensity. The increase in the low-intensity and high-intensity extreme precipitation indices from the RCP8.5 scenario in the late twenty-first century will be distributed in the manner of “south-high-north-low”. In the prediction results of the number of months with an SPI of -1.0 or less, drought months of the NEK sub-region were expected to increase in the two future scenarios in the two future periods. The NEK sub-region includes Gangneung and Sokcho, where large-scale wildfires occur frequently. As the NEK sub-region is expected to increase drought months in all future scenarios, it is necessary to strengthen responses and preventive measures against future wildfire outbreaks. Moreover, it is necessary to investigate the causes of the increase in the future drought months of the NEK sub-region.

This study objectively classified the sub-regions based on the present precipitation characteristics for observations in South Korea, which is smaller than the domain applied by Park et al. (2021). Moreover, by applying the bias correction technique to the RCM, more reliable future precipitation information was presented for precipitation

sub-regions classified in South Korea. The results of this study that intensifying warming will lead to large increases in high-intensity extreme precipitation and mean precipitation intensity in all classified precipitation sub-regions support the possibility that hydrological disasters such as flash floods and landslides in South Korea may increase in the future. Therefore, we expect that this study using the RCM with improved spatial resolution will help prepare practical countermeasures for future precipitation changes over regional and local spatial scales.

Supplementary Information The online version contains supplementary material available at <https://doi.org/10.1007/s13143-022-00292-3>.

Acknowledgements This research was supported by Basic Science Research Program through the National Research Foundation of Korea (NRF) funded by the Ministry of Education (NRF-2019R111A1A01054493), and in part supported by Carbon Neutral Institute Research Fund (Project No. 1.220093.01) of UNIST (Ulsan National Institute of Science & Technology).

Data Availability The data that support the findings of this study are available upon reasonable request from the authors.

References

- Ahn, J.-B., Jo, S., Suh, M.-S., Cha, D.-H., Lee, D.-K., Hong, S.-Y., Min, S.-K., Park, S.-C., Kang, H.-S.: Changes of precipitation extremes over South Korea projected by the 5 RCMs under RCP scenarios. *Asia. Pac. J. Atmos. Sci.* **52**, 223–236 (2016). <https://doi.org/10.1007/s13143-016-0021-0>
- An, S., Park, G., Jung, H., Jang, D.: Assessment of future drought index using SSP scenario in Rep. of Korea. *Sustainability* **14**, 4252 (2022). <https://doi.org/10.3390/su14074252>
- Awan, J., Bae, D.-H., Kim, K.-J.: Identification and trend analysis of homogeneous rainfall zones over the East Asia monsoon region. *Int. J. Climatol.* **35**, 1422–1433 (2015). <https://doi.org/10.1002/joc.4066>
- Barnes, S.L.: A technique for maximizing details in numerical weather map analysis. *J. Appl. Meteorol.* **3**, 396–409 (1964). [https://doi.org/10.1175/1520-0450\(1964\)003%3c0396:ATFMDI%3e2.0.CO;2](https://doi.org/10.1175/1520-0450(1964)003%3c0396:ATFMDI%3e2.0.CO;2)
- Baek, H.-J., Lee, J., Lee, H.-S., et al.: Climate change in the 21st century simulated by HadGEM2-AO under representative concentration pathways. *Asia Pac. J. Atmos. Sci.* **49**, 603–618 (2013). <https://doi.org/10.1007/s13143-013-0053-7>
- Bieniek, P.A., Bhatt, U.S., Thoman, R.L., Angeloff, H., Partain, J., Papineau, J., Fritsch, F., Holloway, E., Walsh, J.E., Daly, C., Shulski, M., Hufford, G., Hill, D.F., Calos, S., Gens, R.: Climate divisions for Alaska based on objective methods. *J. Appl. Meteorol. Climatol.* **51**, 1276–1289 (2012). <https://doi.org/10.1175/JAMC-D-11-0168.1>
- Bothe, O., Fraedrich, K., Zhu, X.: Precipitation climate of Central Asia and the large-scale atmospheric circulation. *Theor. Appl. Climatol.* **108**, 345–354 (2012). <https://doi.org/10.1007/s00704-011-0537-2>
- Cha, D.-H., Lee, D.-K.: Reduction of systematic errors in regional climate simulations of the summer monsoon over East Asia and the western North Pacific by applying the spectral nudging technique. *J. Geophys. Res.* **114**, D14108 (2009). <https://doi.org/10.1029/2008JD011176>



- Cha, D.-H., Lee, D.-K., Jin, C.-S., Kim, G., Choi, Y., Suh, M.-S., Ahn, J.-B., Hong, S.-Y., Min, S.-K., Park, S.-C., Kang, H.-S.: Future changes in summer precipitation in regional climate simulations over the Korean Peninsula forced by multi-RCP scenarios of HadGEM2-AO. *Asia. Pac. J. Atmos. Sci.* **52**, 139–149 (2016). <https://doi.org/10.1007/s13143-016-0015-y>
- Chang, C.H., Ding, Z.K.: Categorical data visualization and clustering using subjective factors. *Data. Knowl. Eng.* **53**, 243–262 (2005). <https://doi.org/10.1016/j.datak.2004.09.001>
- Choi, K.-S., Kim, B.-J.: Climatological characteristics of tropical cyclones making landfall over the Korean peninsula. *J. Korean Meteorol. Soc.* **43**, 97–109 (2007)
- Choi, Y.-W., Ahn, J.-B., Suh, M.-S., Cha, D.-H., Lee, D.-K., Hong, S.-Y., Min, S.-K., Park, S.-C., Kang, H.-S.: Future changes in drought characteristics over South Korea using multi regional climate models with the standardized precipitation index. *Asia Pac. J. Atmos. Sci.* **52**, 209–222 (2016). <https://doi.org/10.1007/s13143-016-0020-1>
- Davies, T., Cullen, M.J.P., Malcolm, A.J., Mawson, M.H., Staniforth, A., White, A.A., Wood, N.: A new dynamical core for the met office's global and regional modeling of the atmosphere. *Q. J. r. Meteorol. Soc.* **131**, 1759–1782 (2005). <https://doi.org/10.1256/qj.04.101>
- Giorgi, F., Jones, C., Asrar, G.R.: Addressing climate information needs at the regional level: the CORDEX framework. *WMO Bull.* **58**, 175–183 (2009)
- Giorgi, F., Coppola, E., Solmon, F., Mariotti, L., Sylla, M.B., Bi, X., Elguindi, N., Diro, G.T., Nair, V., Giuliani, G., Turuncoglu, U.U., Cozzini, S., Guttler, I., O'Brien, T.A., Tawfik, A.B., Shalaby, A., Zakey, A.S., Steiner, A.L., Stordal, F., Sloan, L.C.: RegCM4: model description and preliminary tests over multiple CORDEX domains. *Clim. Res.* **52**, 7–29 (2012). <https://doi.org/10.3354/cr01018>
- Guo, Y., Cao, J., Li, H., Wang, J., Ding, Y.: Simulation of the interface between the Indian summer monsoon and the East Asian summer monsoon: Intercomparison between MPI-ESM and ECHAM5/MPI-OM. *Adv. Atmos. Sci.* **33**, 294–308 (2016). <https://doi.org/10.1007/s00376-015-5073-z>
- Guttman, N.B.: Accepting the standardized precipitation index: a calculation algorithm. *J. Am. Water Resour. Assoc.* **35**, 311–322 (1999)
- Hayes, M.J., Svoboda, M.D., Wilhite, D.A., Vanyarkho, O.V.: Monitoring the 1996 drought using the standardized precipitation index. *Bull. Am. Meteorol. Soc.* **80**, 429–438 (1999). [https://doi.org/10.1175/1520-0477\(1999\)080%3c0429:MTDUTS%3e2.0.CO;2](https://doi.org/10.1175/1520-0477(1999)080%3c0429:MTDUTS%3e2.0.CO;2)
- Hayes, M., Svoboda, M., Wall, N., Widhalm, M.: The Lincoln declaration on drought indices: universal meteorological drought index recommended. *Bull. Am. Meteorol. Soc.* **92**, 485–488 (2011). <https://doi.org/10.1175/2010BAMS3103.1>
- Hong, S.-Y., Park, H., Cheong, H.-B., Kim, J.E.E., Koo, M.-S., Jang, J., Ham, S., Hwang, S.-O., Park, B.-K., Chang, E.-C., Li, H.: The Global/Regional Integrated Model system (GRIMs). *Asia. Pac. J. Atmos. Sci.* **49**, 219–243 (2013). <https://doi.org/10.1007/s13143-013-0023-0>
- Kim, G., Cha, D.-H., Park, C., Lee, G., Jin, C.-S., Lee, D.-K., Suh, M.-S., Ahn, J.-B., Min, S.-K., Hong, S.-Y., Kang, H.-S.: Future changes in extreme precipitation indices over Korea. *Int. J. Climatol.* **38**, e862–e874 (2018). <https://doi.org/10.1002/joc.5414>
- Kim, G., Cha, D.-H., Lee, G., Park, C., Jin, C.-S., Lee, D.-K., Suh, M.-S., Ahn, J.-B., Min, S.-K., Kim, J.: Projection of future precipitation change over South Korea by regional climate models and bias correction methods. *Theor. Appl. Climatol.* **141**, 1415–1429 (2020). <https://doi.org/10.1007/s00704-020-03282-5>
- Kim, G., Cha, D.-H., Park, C., Jin, C.-S., Lee, D.-K., Suh, M.-S., Oh, S.-K., Hong, S.-Y., Ahn, J.-B., Min, S.-K., Kang, H.-S.: Evaluation and projection of regional climate over East Asia in CORDEX-East Asia phase I experiment. *Asia. Pac. J. Atmos. Sci.* **57**, 119–134 (2021). <https://doi.org/10.1007/s13143-020-00180-8>
- Koch, S.E., DesJardins, M., Kocin, P.J.: An interactive Barnes objective map analysis scheme for use with satellite and conventional data. *J. Appl. Meteorol. Climatol.* **22**, 1487–1503 (1983). [https://doi.org/10.1175/1520-0450\(1983\)022%3c1487:AIBOMA%3e2.0.CO;2](https://doi.org/10.1175/1520-0450(1983)022%3c1487:AIBOMA%3e2.0.CO;2)
- Lee, C.W., Park, M.J., Yoo, D.G.: Quantitative determination procedures for regional extreme drought conditions: Application to historical drought events in South Korea. *Atmosphere* **11**, 581 (2020). <https://doi.org/10.3390/atmos11060581>
- Lee, D., Min, S.-K., Jin, J., Lee, J.-W., Cha, D.-H., Suh, M.-S., Ahn, J.-B., Hong, S.-Y., Kang, H.-S.: Joh, M: Thermodynamic and dynamic contributions to future changes in summer precipitation over Northeast Asia and Korea: a multi-RCM study. *Clim. Dyn.* **49**, 4121–4139 (2017a). <https://doi.org/10.1007/s00382-017-3566-4>
- Lee, D., Min, S.-K., Fischer, E., Shiogama, H., Bethke, I., Lierhammer, L., Scinocca, J. F.: Impacts of half a degree additional warming on the Asian summer monsoon rainfall characteristics. *Environ. Res. Lett.* **13**, 044033 (2018).
- Lee, G., Cha, D.-H., Park, C.: Improvement of extreme summer precipitation over South Korea in APHRODITE data. *J. Clim. Res.* **12**, 41–51 (2017b) (in Korean with English abstract). <https://doi.org/10.14383/cr.2017b.12.1.41>
- Lee, J., Kim, Y., Wang, D.: Assessing the characteristics of recent drought events in South Korea using WRF-Hydro. *J. Hydrol.* **607**, 127459 (2022)
- Maraun, D., Shepherd, T., Widmann, M., et al.: Towards process-informed bias correction of climate change simulations. *Nat. Clim. Change* **7**, 764–773 (2017). <https://doi.org/10.1038/nclimate3418>
- Martin, G.M., Bellouin, N., Collins, W.J.: The HadGEM2 family of Met Office Unified Model climate configurations. *Geosci. Model. Dev.* **4**, 723–757 (2011). <https://doi.org/10.5194/gmd-4-723-2011>
- McKee, T. B., Doesken, N. J., Kleist, J.: The relationship of drought frequency and duration to time scale. In: Proceedings of the Eighth Conference on Applied Climatology, Anaheim, California, 17–22 January 1993. Boston, American Meteorological Society, 179–184 (1993).
- Ministry of Environment: Korean Climate Change Assessment Report 2020 - Climate Impact and Adaptation -. Minister of Environment (2020).
- Murtagh, F., Legendre, P.: Ward's hierarchical agglomerative clustering method: Which algorithms implement Ward's criterion? *J. Classif.* **31**, 274–295 (2014)
- Myoung, B., Rhee, J., Yoo, C.: Long-lead predictions of warm season droughts in South Korea using North Atlantic SST. *J. Clim.* **33**, 4659–4677 (2020)
- Oh, S.-G., Suh, M.-S., Lee, Y.-S., Ahn, J.-B., Cha, D.-H., Lee, D.-K., Kang, H.-S.: Projections of high resolution climate changes for South Korea using multiple-regional climate models based on four RCP scenarios. Part 2: precipitation. *Asia. Pac. J. Atmos. Sci.* **52**, 171–189 (2016). <https://doi.org/10.1007/s13143-016-0018-8>
- Park, C., Moon, J.-Y., Cha, E.-J., Yun, W.-T., Choi, Y.: Recent changes in summer precipitation characteristics over South Korea. *J. Korean Geogr. Soc.* **45**, 324–336 (2008). (in Korean with English abstract)
- Park, C., Choi, Y., Yun, W.-T., Moon, J.-Y.: Classification of climate zones in South Korea considering both air temperature and rainfall. *J. Korean Geogr. Soc.* **44**, 1–16 (2009). (in Korean with English abstract)

- Park, C., Cha, D.-H., Kim, G., Lee, G., Lee, D.-K., Suh, M.-S., Hong, S.-Y., Ahn, J.-B., Min, S.-K.: Evaluation of summer precipitation over Far East Asia and South Korea simulated by multiple regional climate models. *Int. J. Climatol.* **40**, 2270–2284 (2020a). <https://doi.org/10.1002/joc.6331>
- Park, C., Kim, G., Shin, S.-W., Cha, D.-H.: Assessment of the uncertainty for future climate change using bias-corrected high-resolution multi-regional climate models over Seoul metropolitan city. *J. Clim. Res.* **15**, 229–242 (2020b) (in Korean with English abstract). <https://doi.org/10.14383/cri.2020b.15.4.229>
- Park, C., Lee, G., Kim, G., Cha, D.-H.: Future changes in precipitation for identified sub-regions in East Asia using bias-corrected multi-RCMs. *Int. J. Climatol.* **41**, 1889–1904 (2021). <https://doi.org/10.1002/joc.6936>
- Sepulchre, P., Sloan, L. S., Fluteau, F.: Modelling the response of Amazonian climate to the uplift of the Andean Mountain range. In: Hoorn C, Weesling F (eds) *Amazonia – Landscape and species evolution: a look into the past*. Wiley-Blackwell, Chichester, (2010). <https://doi.org/10.1002/9781444306408.ch13>
- Skamarock, W. C., Klemp, J. B., Dudhia, J., Gill, D. O., Barker, D. M., Wang, W., Powers, J. G.: A description of the advanced research WRF version 2. NCAR Technical note TN-468+STR, 88 (2005).
- Sperber, K.R., Annamalai, H., Kang, I.-S., Kitoh, A., Moise, A., Turner, A., Wang, B., Zhou, T.: The Asian summer monsoon: an intercomparison of CMIP5 vs. CMIP3 simulations of the late 20th century. *Clim. Dyn.* **41**, 2711–2744 (2013). <https://doi.org/10.1007/s00382-012-1607-6>
- Suh, M.-S., Oh, S.-G., Lee, Y.-S., Ahn, J.-B., Cha, D.-H., Lee, D.-K., Kang, H.-S.: Projections of high resolution climate changes for South Korea using multiple-regional climate models based on four RCP scenarios. Part 1: surface air temperature. *Asia. Pac. J. Atmos. Sci.* **52**, 151–169 (2016). <https://doi.org/10.1007/s13143-016-0017-9>
- Taylor, K.E.: Summarizing multiple aspects of model performance in a single diagram. *J. Geophys. Res.* **106**, 7183–7192 (2001). <https://doi.org/10.1029/2000JD900719>
- Trenberth, K., Dai, A., van der Schrier, G., Jones, P.D., Barichivich, J., Briffa, K.R., Sheffield, J.: Global warming and changes in drought. *Nat. Clim. Change* **4**, 17–22 (2014). <https://doi.org/10.1038/nclimate2067>
- Ward, J.H.: Hierarchical grouping to optimize an objective function. *J. Am. Stat. Assoc.* **58**, 236–244 (1963)
- Wilks, D.: *Statistical methods in the atmospheric sciences*. 3rd edn. Oxford, Academic Press, 627pp (2011).
- WMO: *Standardized Precipitation Index User Guide*. (M. Svoboda, M. Hayes and D. Wood). WMO-No. 1090. Geneva. ISBN 978–92–63–11091–6. 16pp (2012).
- Yan, D., Werners, S.E., Ludwig, F., Huang, H.Q.: Hydrological response to climate change: the Pearl River, China under different RCP scenarios. *J. Hydrol.* **4**, 228–245 (2015). <https://doi.org/10.1016/j.ejrh.2015.06.006>
- Yoo, J. Y, Song, H., Kim, T.-W., Ahn, J.-H.: Evaluation of short-term drought using daily standardized precipitation index and ROC analysis. *J. Kor. Soc. Civ. Eng.* **33**, 1851–1860 (2013) (in Korean with English abstract). <https://doi.org/10.12652/Ksce.2013.33.5.1851>

Publisher's Note Springer Nature remains neutral with regard to jurisdictional claims in published maps and institutional affiliations.

Springer Nature or its licensor holds exclusive rights to this article under a publishing agreement with the author(s) or other rightsholder(s); author self-archiving of the accepted manuscript version of this article is solely governed by the terms of such publishing agreement and applicable law.

